Measurements of the Allen Telescope Array Performance as an Interferometer

David R. DeBoer and Rob Ackermann
November 23, 2003

In radio astronomy, images of the sky utilizing an array of antennas are made by a technique called interferometry. An interferometer measures the delay in the arrival time of a radio wave at two separate antennas. Under ideal circumstances, this delay is strictly a function of the position of the radio source and the relative positions of the two antennas (the baseline, see Figure 1). The measurement is akin to triangulation through a time of arrival method. A shift in the position of the source with respect to the baseline will cause a corresponding change in the delay. It is this property that allows us to reconstruct the image of a radio source with the many baselines of an interferometer such as the ATA.

Using current arrays, these data must be collected over a fairly long period of time in order to gain enough information to make a good image of the sky. The many antennas of the ATA, however, provide so many simultaneously baselines that it is possible to make instantaneous ("snap-shot") images with good fidelity even of very complex regions. This opens a new window for studying the underlying physics of cosmic phenomena and a very efficient means of surveying the universe.

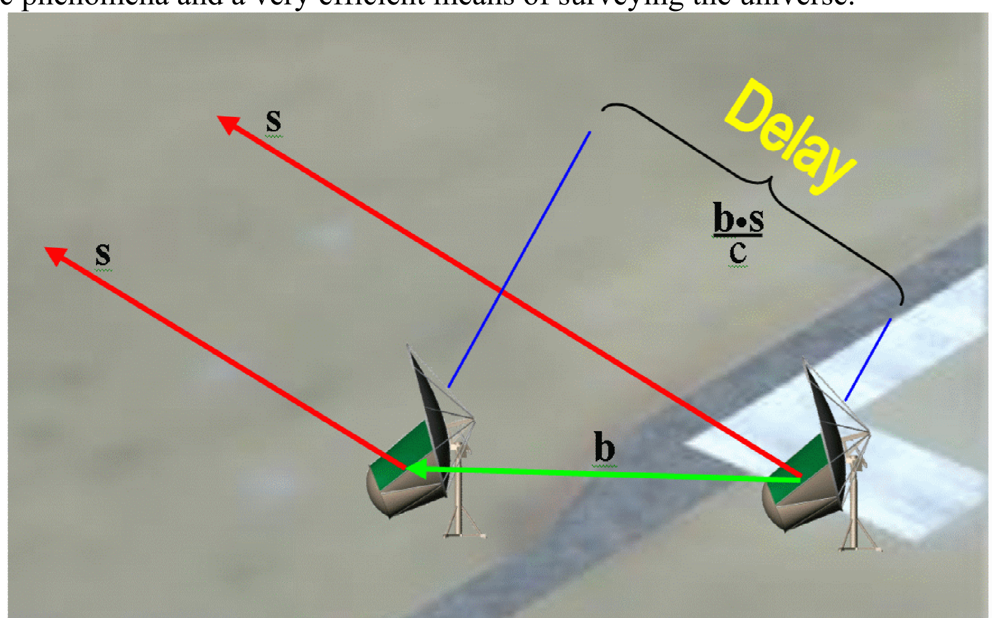

Figure 1: Geometrical delay measured by two offset ATA[1] antennas as an interferometer. An image is constructed by combining a large ensemble of baselines, **b** (*c* is the speed of light), pointing in the direction given by **s**.

[1] Given the offset design, note that the antennas aren't "looking" (shown by the vector **s**) where one might intuit from the geometrical appearance of the antennas.

The relationship between the distribution of signals from the sky and the measured delays between baselines (abstracted to a complex quantity called the "visibility") under conditions applicable to radio astronomy is a Fourier transform expressed as:

$$V(\mathbf{b},\boldsymbol{\sigma}) = \int_S \mathrm{A}(\boldsymbol{\sigma}) I(\boldsymbol{\sigma}) e^{-2\pi i \nu \mathbf{b} \bullet \boldsymbol{\sigma}/c} d\Omega \qquad \text{Eq. 1}$$

where V is the complex visibility, $\mathrm{A}(\boldsymbol{\sigma})$ is the antenna receive pattern, $\boldsymbol{\sigma}$ is the offset from the reference center, $\mathrm{I}(\sigma)$ is the sky brightness temperature distribution, ν is the frequency, and **b** is the baseline vector. The integration is properly over all solid angles; however, practically speaking, the antenna pattern limits the needed integration to near boresight. The interferometer measures a function of the complex visibility, which is then calibrated and transformed to provide the sky brightness temperature distribution, $\mathrm{I}(\sigma)$; the desired image. This procedure is done in a "correlator". The correlator is essentially the equivalent of the lens in a camera. In this case however, it happens last and usually works on digitized data, rather than incident photons.

With this ability to produce radio "pictures" of the sky, one can then apply the data to understanding the underlying astrophysical processes that produce the particular image and spectrum. This is one very important mode of operation of the array. The other mode, which will support SETI as well as a myriad of other users, is to sum the outputs to produce equivalent "pixels-worth" of data, or "beams".

Clearly the ability to collect the signals and combine them in a correlator is a primary ability required of this instrument, and thus several tests have been conducted in order to show the performance of the Allen Telescope Array as an interferometer.

Expected Performance

Knowing the baseline of a measurement, the results of combining the signals may be predicted *a priori*, assuming everything is operating correctly. The baselines of the existing three ATA antennas are shown in Figure 2. As the source moves in the sky, the combined signals from different baselines go in and out of phase (as the delay becomes fractional multiples of a wavelength), resulting in a harmonic signal as a function of time known as a "fringe pattern" (described pictorially in Figure 3). An envelope set by the antenna pattern and the bandwidth modulates the magnitude of this fringe pattern.

The correlator response from a celestially stationary source (where the source appears to move across the sky due to rotation of the earth) will go in and out of phase at a frequency determined by the rotation of the earth (ω_e=7.3×10^{-5} rad/sec), its declination (δ) and the portion of the baseline in the east-west direction (u). The fringe frequency is given by $-\omega_e u \cos\delta$. For the three PTA antennas, that maximum frequency (at, say, 1420 MHz) is about 8.4 ×10^{-3} Hz, or one period roughly every 120 seconds (the maximum E-W baseline is 29.487·cos(35.288°) = 24.07 m, or about 115 wavelengths).

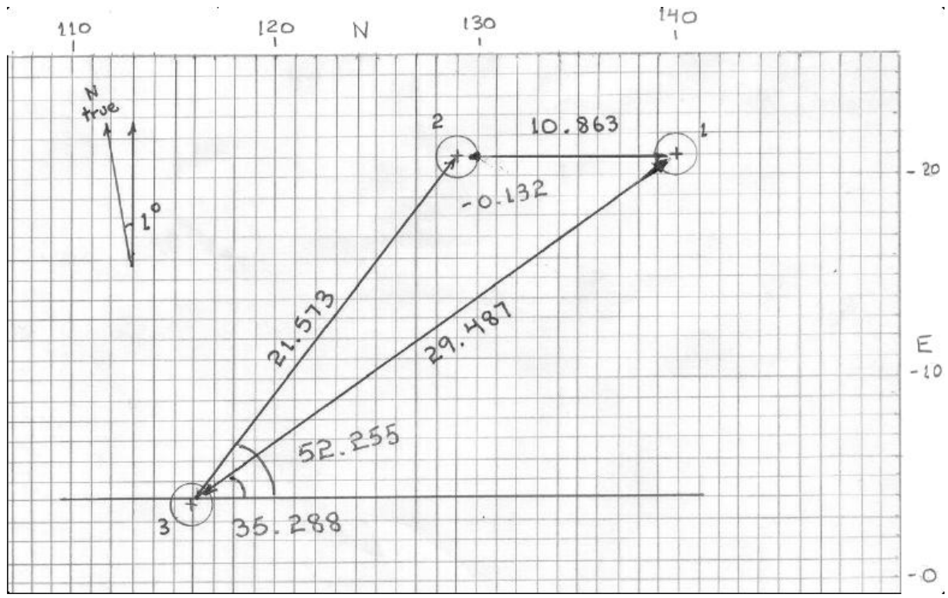

Figure 2: Baselines of the Production Test Array antennas.

Satellites may also be used to measure fringes with the added benefit of strong signals to yield a good signal-to-noise measurement. The GPS satellites provide a particularly good constellation, since the orbital period is sufficiently long (12 hours as seen by an observer rotating with the earth) that tracking is reasonable and there are a lot of them. The GPS orbits are inclined to the earth's axis by 55°. Coincidently, the angle that the longest baseline makes to E-W is roughly the same as the GPS inclination, so, for the three PTA antenna, the maximum fringe frequency is about 2.3×10^{-2} Hz, or one period roughly every 44 seconds. (Note that GPS operates at a frequency of 1575 MHz).

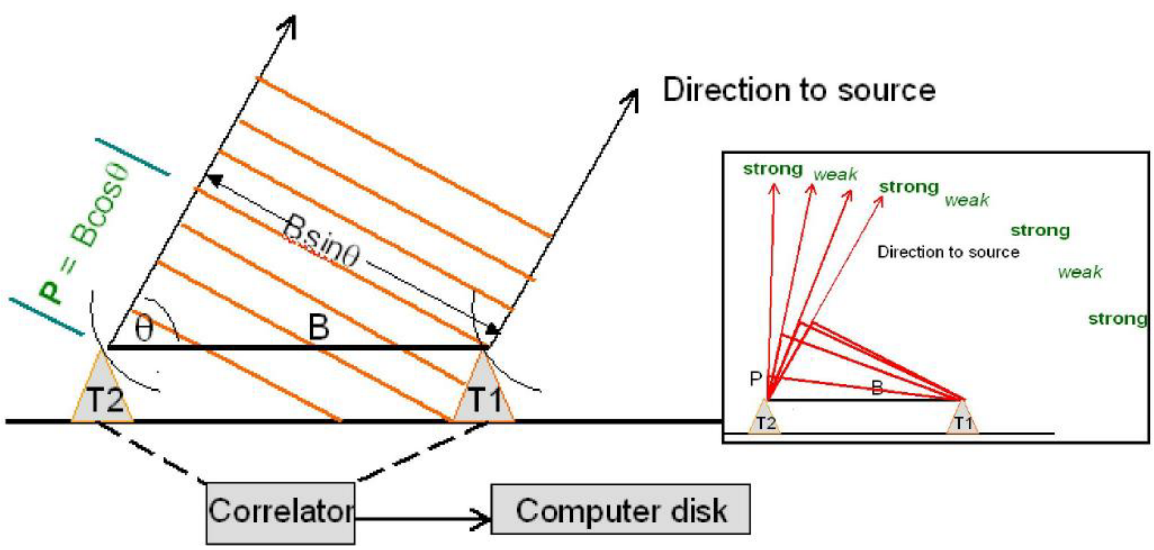

Figure 3: Schematic showing the origin of the fringe pattern. As the location of the source moves relative to the baseline, a sinusoidal interference pattern is generated.

As mentioned earlier, an envelope determined by the bandwidth of the observation and the antenna pattern (unless the source is "tracked" as it moves) modulates the fringe pattern. The ATA antenna has a 3-dB beamwidth given by 3.5°/ν, with ν in GHz, so the beamwidth is traversed in 14 minute-GHz. A GPS satellite will traverse the beam in half that time which, at 1.575 GHz, yields a transit time of 4.4 minutes.

The bandwidth also imposes an envelope that is the Fourier transform of the bandpass filter. Assuming a rectangular filter of bandwidth Δν, the envelope is a "sinc" function, yielding an envelope with a full-width half-max (FWHM) in seconds of time of

$$FWHM = 4\varsigma \sin^{-1}\left[\frac{0.6033c}{D\Delta\nu}\right] \quad \text{sec} \qquad \text{Eq. 2}$$

where the arcsine is in degrees, and ζ is a multiplier to allow different tracking rates. For GPS ζ=1 and for celestially stationary source ζ=2. For GPS (Δν~10MHz, D~29 m) this is about 150 minutes, so the antenna beam pattern will dominate the envelope of the fringe in the non-tracking (or "drift-scan") case.

A given number of antennas (N) has a complement of $N(N-1)/2$ such baselines, which are then used to generate the image from the sky. For any three antennas of an array, the phases due to the geometry of the baseline between these three baselines (3×[3-1]/2 = 3 baselines) must satisfy a constraint called "phase closure". The phase closure condition is that the phases of an unresolved point source (which the GPS satellite satisfies) must sum to zero in a working interferometer (see, for example, Thompson, Moran and Swenson, *Interferometry and Synthesis in Radio Astronomy 2nd Edition*, Wiley-Interscience, 2001).

Results

The three antennas have been undergoing testing for about one year, with the first fringe results obtained in December 2002 using an analog correlator connected by coaxial cable near the antennas. Currently the signals are brought back to the main lab via the production fiber-optic transmitter-receiver units using the controllable production post-amplifier module (PAM). The signals are then digitized and combined in a software correlator. As such, this system represents functionally the same signal path as the production system, and in fact uses the production version of most of the analog signal path. For recent experiments, antenna 1 uses an ATA feed while antennas 2 and 3 use RPA feeds (see Memo3). Figure 4 shows the track of the GPS satellite on August 28, 2003 used to test the interferometer.

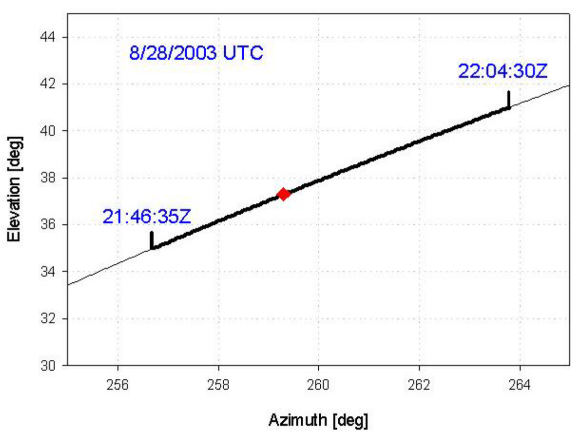

Figure 4: Track of GPS BIIA-15 (PRN) on August 28, 2003 used to test the interferometer. The diamond is at 21:54:29Z, which is 1300 s in the following plots.

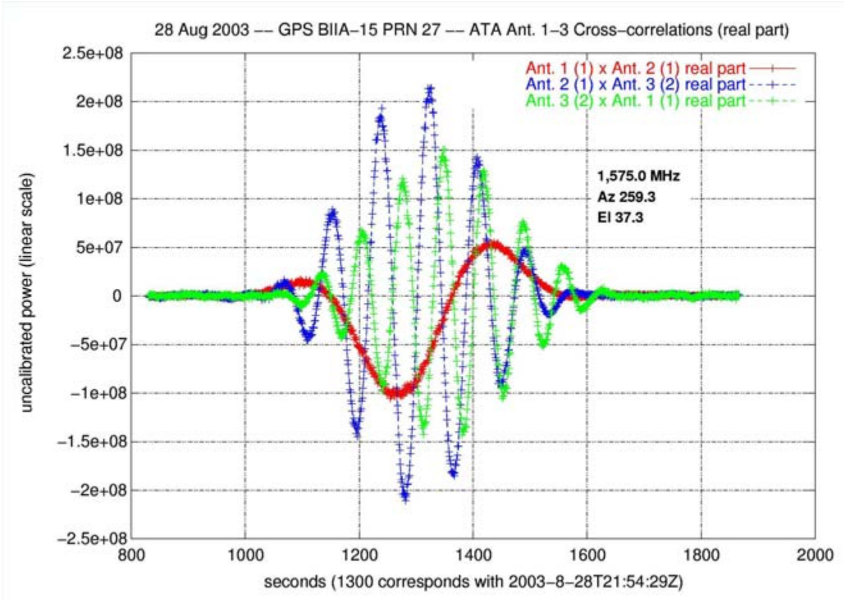

Figure 5: Digital correlator output for the three PTA baselines for GPS drifting through the beams.

The measured fringe patterns are shown in Figure 5 and the predicted fringe periods are shown in Figure 6, with the predicted and measured values near boresight (~1300 s) listed in Table I. The envelope FWHM is about 4.4 minutes. These data yield appropriate fringes on the three baselines, demonstrating that the antennas and feed systems are working properly. Note that the envelope and period for Ant 1*Ant 2 have increased uncertainty due to the long period relative to the envelope width and the lack of a pointing model at this point in the development when these data were obtained. The visibility phases are plotted in Figure 7, clearly showing that the phase closure condition is satisfied.

Table I

Baseline	Measured		Predicted
	Frequency [Hz]	Period [s]	Period [s]
Ant 1 × Ant 2	$\sim 2.4\times10^{-3}$	330-500	415
Ant 2 × Ant 3	1.1×10^{-2}	91	91
Ant 1 × Ant 3	1.3×10^{-2}	75	75

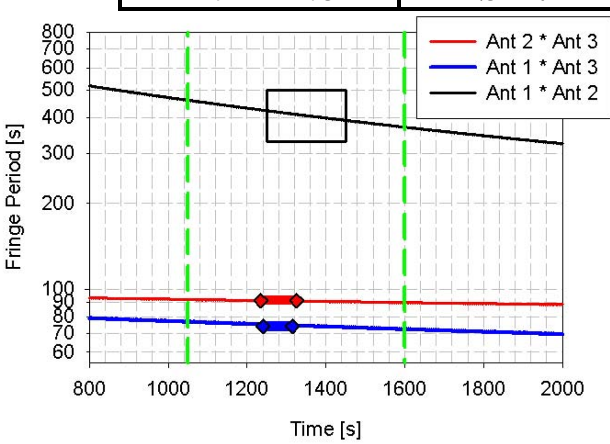

Figure 6: Fringe period measured vs. predicted. The thinner black, red and blue lines are the predicted instantaneous periods, while the black box bounds the measured value for A1*A2 and the thick red and blue lines with diamond ends are the measured periods for the other two baselines, measured over the indicated period.

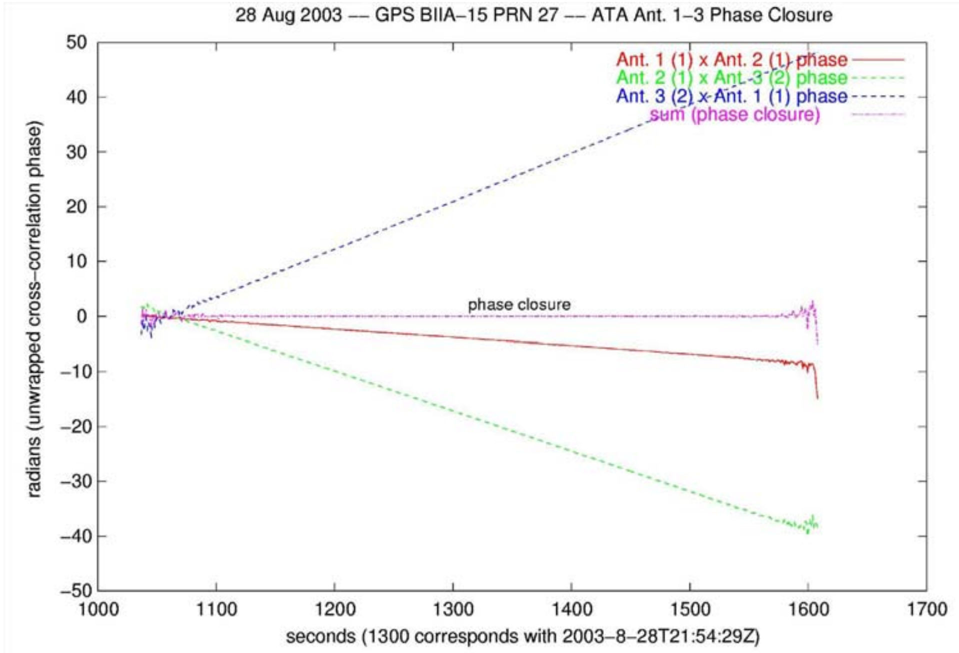

Figure 7: Phases of the visibilities of the three ATA baselines, demonstrating phase closure.

Conclusion

Data from the ATA have been used to demonstrate the functionality of the three existing antennas and baselines as an interferometer. The current data path is functionally equivalent to the final production signal path at all frequencies (since the same hardware is used at all frequencies) and in fact uses the production components for most of the analog signal path. The phase closure condition is shown to be satisfied for observations of a GPS satellite and the fringe frequencies and envelope are consistent with the expected values.